Polymer Bulletin (2019) 76:3297–3327
https://doi.org/10.1007/s00289-018-2543-3

ORIGINAL PAPER

A new synthesis of limonene copolymer: experimental and theoretical analysis

Nevin Cankaya[1] · Emine Tanış[2] · H. Elmalı Gülbaş[3] · Niyazi Bulut[4]

Received: 2 June 2018 / Revised: 9 September 2018 / Accepted: 24 September 2018 /
Published online: 1 October 2018

Abstract

A copolymer of limonene with 2-(4-methoxyphenylamino)-2-oxoethyl methacrylate (LIM-co-MPAEMA) which is thought to be a non-toxic and used generally as a dietary supplement was synthesized and characterized for the first time both experimentally and theoretically. The structure of synthesized limonene copolymer was chemically characterized by Fourier transform infrared and nuclear magnetic resonant (^{1}H NMR) spectroscopic techniques and compared with the theoretical calculated results. Charge transfer that is important in the formation of chemically bonded adducts causing cancer is quantitatively calculated. It was found that this polymer can be used as a biomaterial.

Keywords 2-(4-Methoxyphenylamino)-2-oxoethyl methacrylate (MPAEMA) · Limonene · LIM-co-MPAEMA · Density functional theory (DFT)

Introduction

Polymers today occupy an important place in our lives due to their low cost, durability, chemical resistance and easy availability. Polymers are macromolecules formed by the combination of small units called monomers [1]. If the polymer chains are composed of a single monomer, then homopolymer of these polymers is called copolymers if they consist of different monomers. Copolymerization is a highly effective method for synthesizing products with industrially sought chemical and physical properties, and the structure–property relationship in the copolymerization studies is one of the most investigated. The largest source of raw materials for

✉ Emine Tanış
eminetanis@yandex.com

[1] Department of Chemistry, University of Usak, Usak, Turkey

[2] Kaman Vocational School, Ahi Evran University, Kırsehir, Turkey

[3] Chemical Technology, Usak University, Usak, Turkey

[4] Department of Physics, Firat University, Elazıg, Turkey

synthetic polymers is oil and petroleum derivatives. Rapid decline in oil resources leads to a decrease in oil-based polymer raw material resources and an increase in cost. Therefore, the use of sustainable polymers from natural sources has become very important nowadays, and scientific studies have been directed toward this direction, since these natural polymers have excellent properties such as biocompatibility, non-toxicity, biological degradability and adsorption properties.

One of the most important of the sustainable natural polymer sources is terpenes, which occupy a very large area in organic compounds, which can be obtained from very different sources such as various plants, some insects, fungi and marine microorganisms. Many of the terpenes are isoprene derivatives. Terpenes are known as functional monomers which have commercial importance in the synthesis of homopolymer and copolymer due to their functional groups and their being optically active. Limonene is an optically active monocyclic terpene, found in many citrus fruits. The annual worldwide production of limonene is over 70 million kg [2]. It has been described that it is an important non-toxic substance both in vitro and in vivo studies [3, 4]. Today, limonene as an alternative to many solvents, it is reliably used in industry, such as cosmetics, food industry, medicine and cleaning agents [5–7]. Because of structural two double bonds in the limonene molecules a more sustainable structure for the copolymers can be formed. Polymeric materials have a considerable place in our daily lives because of their various properties such as low cost, chemical resistance and easily manufactural. However, due to the petroleum-based sources of polymer raw materials, the limited availability of these oil resources creates problems in terms of cost and sustainability in the production of these materials. For this reason, sustainable polymer degradation from natural sources such as terpenes has become important in terms of scientific work. Limonene is also an important work area for natural polymer resources [8]. First limonene synthesized by Marvel et al. [9] and Robert and Day [10] and using Friedel–Craft catalyst and Ziegler–Natta catalyst and, then it was copolymerized with maleic anhydride by Douchi et al. [11]. Later, Sritavtava et al. reported the synthesis and characterization copolymerization of limonene with methyl methacrylate [12], styrene [13] and acrylonitrile [14]. Zhang and Dube [15] reported the high concentration of high molecular weight by determining the reactivity ratios of the limonene/butyl methacrylate copolymer.

In a recent study [16], it was claimed that limonene could be a new key to environmentally friendly polymers. In this study, it was shown that it is possible that limonene could be used instead of bisphenol A, which is the potential carcinogen in the polycarbonates found in countless products. They also demonstrated that new limonene-derived biomaterial (poly(limonene)dicarbonate) has the maximum glass transition temperature observed up to now. When the LIM-co-MPAEMA natural polymer is used as a biomaterial, that is, when it interacts with a biosystem, the investigation of the toxic potential is an important consideration. Efforts to determine the toxic potential of various compounds, from small molecules to biosystems, are a large part of toxicity studies [17–19]. In this context, recent studies have shown that the DFT-based reactivity descriptors are advantageous and can be compared with the experimental observations [20]. The reactivity descriptors calculated using the DFT method play an important and reliable role in many studies [21–32]. Global

hardness (η), electrophilicity index (ω), chemical potential (μ) and electronegativity (χ) are a few examples of these reactivity indicators. In addition, toxicity is thought to result from possible transfer of charge between a toxin and a biosystem [21, 33, 34]. Here, a model biosystem has been constructed from selective nucleic acid (NA) bases, since a toxin is expected to interact with NA bases.

In this study, the copolymer of methacrylate derivative 2-(4-methoxyphenylamino)-2-oxoethyl methacrylate (MPAEMA) monomer with a natural monomer–limonene has been synthesized for investigation of structure–property relationship in the limonene copolymer. The limonene copolymer was characterized by classic spectroscopic methods (FTIR, ^{1}H-NMR). Meth/acrylates are very important in the production of polymeric materials due to their chemical and physical properties [35–37]. In recent years, a lot of studies on limonene- and methacrylate-based polymers are available. However, vibration wave numbers, electronic properties, molecular electrostatic potential and chemical shifts are not yet available. This lack of literature encouraged us to determine many physical and chemical properties of this polymer. We have been calculated the amount of charge transfer between a model biosystem and a LIM-co-MPAEMA molecule, which is thought to be non-toxic, to have information about toxic behavior in a biosystem using HOMO–LUMO energy values. We chose nucleic acid (NA) bases (adenine, thymine, cytosine, uracil and guanine), as a model of biomolecules in this study.

Experimental

Materials and methods

Triethylamine, p-methoxyaniline, chloroacetyl chloride, sodium methacrylate, Tebax, NaI, D-limonene, 2,2′-azobisisobutyronitrile (AIBN) and hydroquinone were purchased from Aldrich Chemical Reagent CO. Ltd. 1,4-Dioxane was purchased from Merck Chemical Reagent CO. Ltd. All the solid chemicals were used as received without further purification. All solvents were distilled under vacuum.

Measurements

Fourier transform infrared (FTIR) studies were performed by ATR equipment using Perkin-Elmer FTIR spectroscope. The scanned wave numbers range from 4000 to 400 cm^{-1}. ^{1}H-NMR measurements was taken on Bruker 400 MHz in $CDCl_3$ as solvent with tetramethylsilane (TMS) as the internal reference. The molecular weight of the LIM-co-MPAEMA was determined by using gel permeation chromatography (GPC) on Waters 996 apparatus equipped with evaporative mass detector, $CHCl_3$ solvent with polystyrene standards. Thermal analyzation of the LIM-co-MPAEMA was obtained with a Hitachi 7000 TGA/DTG (thermogravimetric analysis/derivative thermal gravimetric analysis) simultaneous system and a heating rate of 10 °C min^{-1} in nitrogen atmosphere, from 40 to 550 °C temperatures.

Synthesis of LIM-co-MPAEMA

MPAEMA monomer was synthesized and characterized in the presence of p-methoxyaniline, triethylamine, chloroacetyl chloride, sodium methacrylate, Tebax and NaI in our laboratory [38]. The two appropriate monomers, MPAEMA (1 mmol) and D-limonene (1 mmol), with the radical initiator AIBN in 1,4-dioxane solution were added into polymerization flask. The system was kept under inert gas at 70 °C in 24 h. The resulting copolymer was crystallized 3 times to remove impurities with ethyl alcohol. Synthesis of limonene with MPAEMA (LIM-co-MPAEMA) is shown in Fig. 1a and b, respectively. The chemical structure of LIM-co-MPAEMA was characterized by spectroscopic methods (FTIR, ^{1}H-NMR) [39].

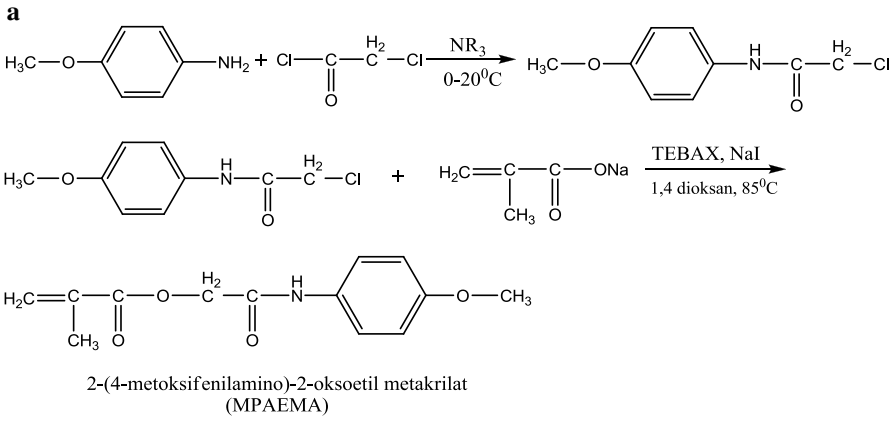

Fig. 1 **a** Synthesis of MPAEMA. **b** Synthesis reaction of LIM-co-MPAEMA

Theoretical calculations

The geometrical, spectroscopic and electronic properties of LIM-co-MPAEMA have been investigated using DFT [40] at the B3LYP level [41–43]. The 6-311G++(d,p) basis set has been used in the calculations. The calculations have been performed using the GAUSSIAN09 program [44]. The optimized geometric parameters (bond lengths, bond angles and dihedral angles) are given in Table 1. The optimized structural parameters were used in calculating vibrational frequency and isotropic chemical shift. In order to make the calculated vibrational frequencies more compliant with the experimental results, they were multiplied by 0.935 [45] as a global scaling factor for B3LYP/6-311++G(d,p). Vibrational modes were assigned through VEDA4 program [46]. Later, TD-DFT method used to get maximum wavelengths, HOMO, LUMO and other electronic properties, such as chemical hardness, chemical potential, electronegativity, and electrophilicity index in different solvents. HOMO and LUMO orbitals are used to find ionization energy and electron affinity, namely $I = -\mathrm{E}_{\mathrm{HOMO}}$, $A = -\mathrm{E}_{\mathrm{LUMO}}$, $\eta = (\mathrm{I} - A)/2$ and $\mu = (\mathrm{I} + A)/2$.

Interaction between the compounds and NA bases (adenine, thymine, cytosine, uracil and guanine) has been determined using the parameter ΔN transferred from a system A to system B and is represented by Parr formula [47]:

$$\Delta N = \frac{\mu_B - \mu_A}{2(\eta_A + \eta_{B)}} \tag{1}$$

^{1}H and ^{13}C NMR isotropic chemical shifts were calculated via GIAO [48, 49] with the basis set of B3LYP/6-311++G(d,p) in DMF (N,N-dimethylformamide), acetonitrile, chloroform solvents. GaussSum2.2 program [50] was used to analyze the spectra of the total density of state (TDOS or DOS), partial density of state (PDOS) overlap population density of states (OPDOS or COOP) and the group contributions of molecular orbitals.

Results and discussion

Spectroscopic characterization of LIM-co-MPAEMA with vibrational frequencies and infrared spectra

The reaction scheme for the synthesis of copolymer LIM-co-MPAEMA is given in Fig. 1. The synthesis of copolymer LIM-co-MPAEMA was carried out by free radical polymerization of MPAEMA and D-limonene in the preference of AIBN as an initiator.

Optimized ground-state structure of LIM-co-MPAEMA with atom numbering calculated by B3LYP/6-311++G(d,p) is shown in Fig. 2. The chemical structure of the LIM-co-MPAEMA was confirmed by FTIR and ^{1}H-NMR. The recommended structure is in full agreement with all spectroscopic data. Measured and calculated FTIR spectrum of the copolymer LIM-co-MPAEMA is shown in Fig. 3. The theoretical vibrational frequencies are multiplied by the

Table 1 Some geometrical parameters optimized in LIM-co-MPAEMA [bond length (Å) and bond angle (°)]

	Limonen
Bond length	
C1–C2	1.40
C1–C6	1.40
C1–O29	1.39
C2–C3	1.39
C2–H7	1.08
C3–C4	1.41
C3–H8	1.08
C4–C5	1.40
C4–N11	1.42
C5–C6	1.40
C5–H9	1.08
C6–H10	1.08
N11–H12	1.01
N11–C13	1.36
C13–O14	1.25
C13–C15	1.52
C15–H16	1.09
C15–H17	1.09
C15–O18	1.47
O18–C20	1.39
O19–C20	1.23
C20–C21	1.53
C21–C22	1.56
C21–C30	1.54
C21–C34	1.55
C22–H23	1.09
C22–H24	1.09
C22–C60	1.56
C25–H26	1.09
C25–H27	1.09
C25–H28	1.08
C25–029	1.45
C30–H31	1.09
C30–H32	1.09
C30–H33	1.09
C34–H35	1.09
C34–H36	1.09
C34–H37	1.09
C38–C39	1.54
C38–C40	1.54
C38–H41	1.10
C38–C60	1.56

Table 1 (continued)

	Limonen
C39–C42	1.54
C39–H43	1.09
C39–H44	1.09
C40–C45	1.51
C40–H46	1.10
C40–H47	1.10
C42–C48	1.52
C42–H49	1.10
C42–H55	1.10
C45–C48	1.34
C45–H50	1.09
C48–C51	1.51
C51–H52	1.09
C51–H53	1.10
C51–H54	1.10
C56–H57	1.09
C56–H58	1.09
C56–H59	1.09
C56–C60	1.54
C60–H61	1.10
Bond angles	
C2–C1–C6	119.75
C2–C1–O29	115.73
C6–C1–O29	124.52
C1–C2–C3	120.89
C1–C2–H7	118.37
C3–C2–H7	120.75
C2–C3–C4	119.71
C2–C3–H8	120.85
C4–C3–H8	119.44
C3–C4–C5	119.16
C3–C4–N11	123.17
C5–C4–N11	117.67
C4–C5–C6	121.04
C4–C5–H9	119.82
C6–C5–H9	119.14
C1–C6–C5	119.45
C1–C6–H10	121.35
C5–C6–H10	119.20
C4–N11–H12	116.76
C4–N11–C13	128.62
H12–N11–C13	114.62
N11–C13–O14	125.92

Table 1 (continued)

	Limonen
N11–C13–C15	115.63
O14–C13–C15	118.44
C13–C15–H16	109.65
C13–C15–H17	109.75
C13–C15–O18	109.86
H16–C15–H17	108.25
H16–C15–O18	109.57
H17–C15–O18	109.74
C15–O18–C20	117.45
O18–C20–O19	120.94
O18–C20–C21	112.41
O19–C20–C21	126.65
C20–C21–C22	109.37
C20–C21–C30	108.67
C20–C21–C34	108.77
C22–C21–C30	111.60
C22–C21–C34	108.97
C30–C21–C34	109.41
C21–C22–H23	106.69
C21–C22–H24	107.53
C21–C22–C60	116.06
H23–C22–H24	106.34
H23–C22–C60	110.08
H24–C22–C60	109.67
H26–C25–H27	109.73
H26–C25–H28	109.60
H26–C25–O29	111.32
H27–C25–H28	109.58
H27–C25–O29	111.36
H28–C25–O29	105.15
C1–O29–C25	118.94
C21–C30–H31	109.49
C21–C30–H32	110.76
C21–C30–H33	111.87
H31–C30–H32	108.54
H31–C30–H33	108.79
H32–C30–H33	107.30
C21–C34–H35	111.04
C21–C34–H36	109.34
C21–C34–H37	111.42
H35–C34–H36	108.01
H35–C34–H37	108.36
H36–C34–H37	108.57

Table 1 (continued)

	Limonen
C39–C38–C40	109.28
C39–C38–H41	107.01
C39–C38–C60	114.43
C40–C38–H41	106.61
C40–C38–C60	112.72
H41–C38–C60	106.30
C38–C39–C42	110.83
C38–C39–H43	109.32
C38–C39–H44	110.92
C42–C39–H43	108.99
C42–C39–H44	109.82
H43–C39–H44	106.87
C38–C40–C45	112.61
C38–C40–H46	110.15
C38–C40–H47	109.26
C45–C40–H46	109.53
C45–C40–H47	109.50
H46–C40–H47	105.54
C39–C42–C48	112.89
C39–C42–H49	109.74
C39–C42–H55	109.99
C48–C42–H49	109.30
C48–C42–H55	109.12
H49–C42–H55	105.54
C40–C45–C48	124.58
C40–C45–H50	116.34
C48–C45–H50	119.08
C42–C48–C45	121.40
C42–C48–C51	116.06
C45–C48–C51	122.54
C48–C51–H52	111.68
C48–C51–H53	111.07
C48–C51–H54	111.25
H52–C51–H53	107.89
H52–C51–H54	108.04
H53–C51–H54	106.70
H57–C56–H58	107.44
H57–C56–H59	107.52
H57–C56–C60	110.72
H58–C56–H59	107.92
H58–C56–C60	111.87
H59–C56–C60	111.17
C22–C60–C38	111.33

Table 1 (continued)

	Limonen
C22–C60–C56	111.18
C22–C60–H61	107.96
C38–C60–C56	113.30
C38–C60–H61	105.63
C56–C60–H61	107.05
Dihedral angles	
C6–C1–C2–C3	0.04
C6–C1–C2–H7	179.99
O29–C1–C2–C3	− 179.92
O29–C1–C2–H7	0.02
C2–C1–C6–C5	− 0.05
C2–C1–C6–H10	− 179.99
O29–C1–C6–C5	179.91
O29–C1–C6–H10	− 0.03
C2–C1–O29–C25	179.40
C6–C1–O29–C25	− 0.57
C1–C2–C3–C4	− 0.01
C1–C2–C3–H8	179.81
H7–C2–C3–C4	− 179.96
H7–C2–C3–H8	− 0.13
C2–C3–C4–C5	0.00
C2–C3–C4–N11	− 179.91
H8–C3–C4–C5	− 179.83
H8–C3–C4–N11	0.27
C3–C4–C5–C6	− 0.01
C3–C4–C5–H9	179.82
N11–C4–C5–C6	179.90
N11–C4–C5–H9	− 0.27
C3–C4–N11–H12	178.64
C3–C4–N11–C13	− 2.09
C5–C4–N11–H12	− 1.27
C5–C4–N11–C13	178.01
C4–C5–C6–C1	0.04
C4–C5–C6–H10	179.97
H9–C5–C6–C1	− 179.79
H9–C5–C6–H10	0.14
C4–N11–C13–O14	0.28
C4–N11–C13–C15	− 179.68
H12–N11–C13–O14	179.56
H12–N11–C13–C15	− 0.39
N11–C13–C15–H16	120.24
N11–C13–C15–H17	− 120.98
N11–C13–C15–O18	− 0.23

Table 1 (continued)

	Limonen
O14–C13–C15–H16	– 59.72
O14–C13–C15–H17	59.07
O14–C13–C15–O18	179.81
C13–C15–O18–C20	– 174.23
H16–C15–O18–C20	65.25
H17–C15–O18–C20	– 53.48
C15–O18–C20–O19	– 0.03
C15–O18–C20–C21	179.98
O18–C20–C21–C22	– 59.78
O18–C20–C21–C30	178.17
O18–C20–C21–C34	59.14
O19–C20–C21–C22	120.23
O19–C20–C21–C30	– 1.82
O19–C20–C21–C34	– 120.85
C20–C21–C22–H23	178.44
C20–C21–C22–H24	64.69
C20–C21–C22–C60	– 58.50
C30–C21–C22–H23	– 61.28
C30–C21–C22–H24	– 175.03
C30–C21–C22–C60	61.77
C34–C21–C22–H23	59.66
C34–C21–C22–H24	– 54.09
C34–C21–C22–C60	– 177.28
C20–C21–C30–H31	179.98
C20–C21–C30–H32	– 60.35
C20–C21–C30–H33	59.30
C22–C21–C30–H31	59.29
C22–C21–C30–H32	178.96
C22–C21–C30–H33	– 61.38
C34–C21–C30–H31	– 61.39
C34–C21–C30–H32	58.27
C34–C21–C30–H33	177.93
C20–C21–C34–H35	60.11
C20–C21–C34–H36	179.20
C20–C21–C34–H37	– 60.78
C22–C21–C34–H35	179.27
C22–C21–C34–H36	– 61.64
C22–C21–C34–H37	58.38
C30–C21–C34–H35	– 58.46
C30–C21–C34–H36	60.63
C30–C21–C34–H37	– 179.35
C21–C22–C60–C38	127.34
C21–C22–C60–C56	– 105.30

Table 1 (continued)

	Limonen
C21–C22–C60–H61	11.83
H23–C22–C60–C38	– 111.39
H23–C22–C60–C56	15.97
H23–C22–C60–H61	133.10
H24–C22–C60–C38	5.27
H24–C22–C60–C56	132.63
H24–C22–C60–H61	– 110.24
H26–C25–O29–C1	– 60.98
H27–C25–O29–C1	61.82
H28–C25–O29–C1	– 179.58
C40–C38–C39–C42	61.47
C40–C38–C39–H43	– 58.68
C40–C38–C39–H44	– 176.27
H41–C38–C39–C42	– 53.61
H41–C38–C39–H43	– 173.76
H41–C38–C39–H44	68.65
C60–C38–C39–C42	– 171.08
C60–C38–C39–H43	68.77
C60–C38–C39–H44	– 48.82
C39–C38–C40–C45	– 44.68
C39–C38–C40–H46	77.91
C39–C38–C40–H47	– 166.59
H41–C38–C40–C45	70.65
H41–C38–C40–H46	– 166.76
H41–C38–C40–H47	– 51.26
C60–C38–C40–C45	– 173.09
C60–C38–C40–H46	– 50.50
C60–C38–C40–H47	65.00
C39–C38–C60–C22	71.67
C39–C38–C60–C56	– 54.53
C39–C38–C60–H61	– 171.39
C40–C38–C60–C22	– 162.65
C40–C38–C60–C56	71.15
C40–C38–C60–H61	– 45.72
H41–C38–C60–C22	– 46.21
H41–C38–C60–C56	– 172.40
H41–C38–C60–H61	70.73
C38–C39–C42–C48	– 46.16
C38–C39–C42–H49	– 168.34
C38–C39–C42–H55	75.98
H43–C39–C42–C48	74.19
H43–C39–C42–H49	– 48.00
H43–C39–C42–H55	– 163.68

Table 1 (continued)

	Limonen
H44–C39–C42–C48	– 169.05
H44–C39–C42–H49	68.76
H44–C39–C42–H55	– 46.92
C38–C40–C45–C48	14.34
C38–C40–C45–H50	– 165.13
H46–C40–C45–C48	– 108.59
H46–C40–C45–H50	71.93
H47–C40–C45–C48	136.12
H47–C40–C45–H50	– 43.36
C39–C42–C48–C45	14.82
C39–C42–C48–C51	– 165.63
H49–C42–C48–C45	137.25
H49–C42–C48–C51	– 43.20
H55–C42–C48–C45	– 107.80
H55–C42–C48–C51	71.75
C40–C45–C48–C42	1.39
C40–C45–C48–C51	– 178.14
H50–C45–C48–C42	– 179.15
H50–C45–C48–C51	1.33
C42–C48–C51–H52	– 178.03
C42–C48–C51–H53	– 57.54
C42–C48–C51–H54	61.17
C45–C48–C51–H52	1.52
C45–C48–C51–H53	122.01
C45–C48–C51–H54	– 119.28
H57–C56–C60–C22	59.65
H57–C56–C60–C38	– 174.07
H57–C56–C60–H61	– 58.04
H58–C56–C60–C22	179.47
H58–C56–C60–C38	– 54.26
H58–C56–C60–H61	61.77
H59–C56–C60–C22	– 59.80
H59–C56–C60–C38	66.48
H59–C56–C60–H61	– 177.49

scaling factors of 0.935 for DFT/B3LYP/6-311++G(d,p) to compare the theoretical vibrational frequencies with the experimental ones. As seen from the correlation graph (Fig. 4), the correlation coefficient is 0.999. At the same time, the theoretical wave numbers and the potential energy distributions (PED values) of the vibrational modes for headline polymer are listed in Table 2, in comparison with the observed vibrational spectra of this molecule.

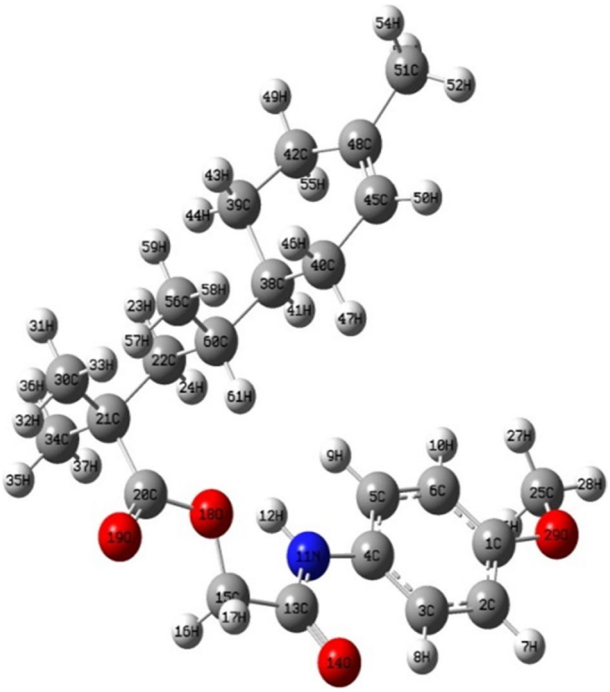

Fig. 2 Optimized geometric structures of LIM-co-MPAEMA

N–H aromatic stretch appears at 3390 ± 60 cm^{-1} [51]. N–H stretching frequency was observed at 3317 cm^{-1} and calculated as 3368 cm^{-1}. The contribution of PED of N–H band was 100%. C=O stretching vibration was observed in the range 1850–1550 cm^{-1} [52]. In this study, C=O ester band was recorded at 1736 cm^{-1}. The calculated scaled frequency at 1673 cm^{-1} and its contribution of PED was 90%. O=C–NH amide stretch was observed 1678 cm^{-1} and calculated 1633 cm^{-1}. C=C stretches on aromatic ring which are not significantly influenced by the nature of the substituents are expected in the region 1650–1100 cm^{-1} [53]. The C=C stretching vibrations of title molecule were observed 1538 and 1603 cm^{-1}. They were calculated 1550 and 1614 cm^{-1}. It is seen that there is a great deal of agreement between the experimental and theoretical IR data in Table 2.

Spectroscopic characterization of LIM-co-MPAEMA with ^{1}H-NMR

The isotropic chemical shifts were used in the identification of ionic species and reactive organic. ^{1}H NMR spectra were obtained on a Bruker 400 MHz

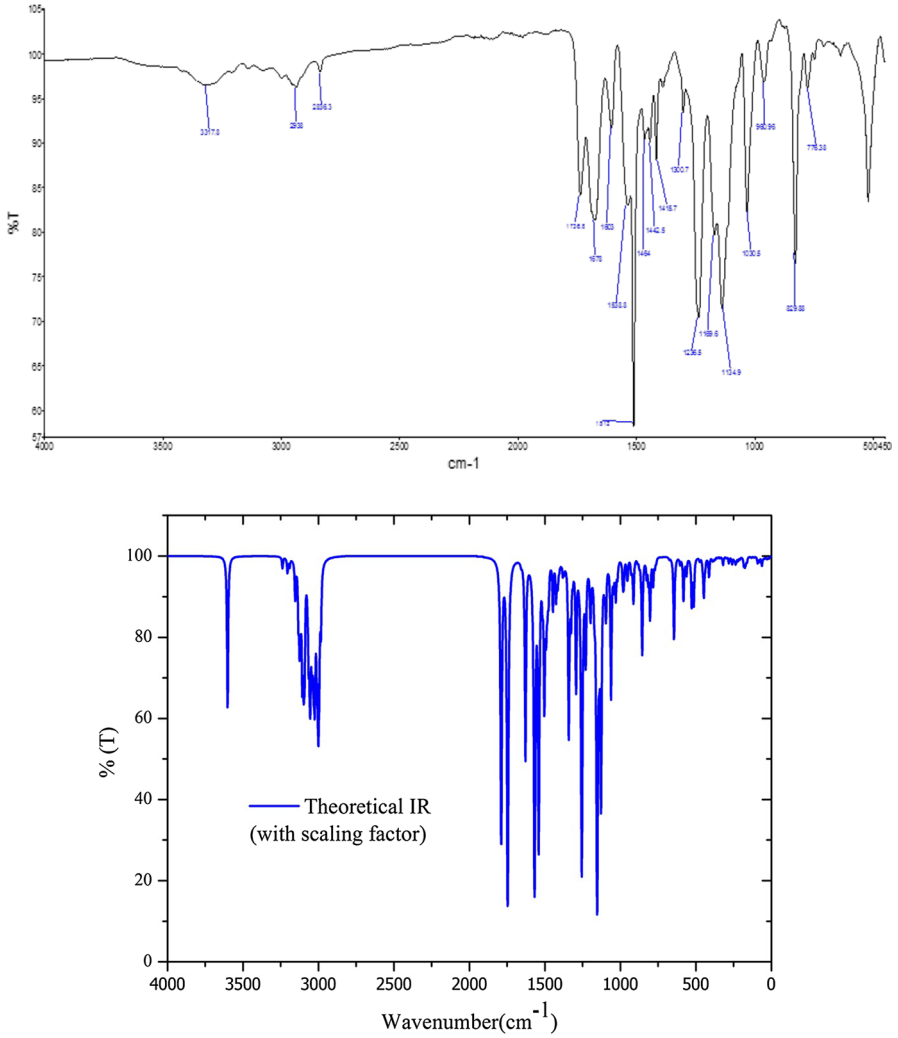

Fig. 3 Experimental and theoretical FTIR spectra of LIM-co-MPAEMA

spectrometer in chloroform and ^{1}H and ^{13}C chemical shifts were calculated in DMF, acetonitrile and chloroform solvents by using the gauge-independent atomic orbital (GIAO) method at B3LYP/6-311++G(d,p) level of theory, as depicted in Table 3. TMS was considered internal reference. The numbering of the atoms has been determined as in Fig. 2. The experimental ^{1}H spectra are

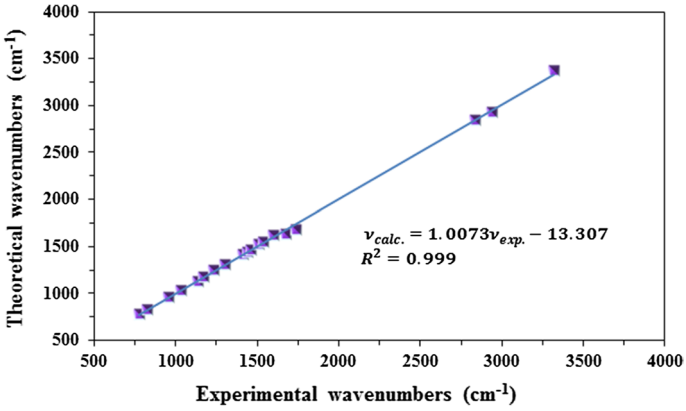

Fig. 4 Correlation graphic of calculated and experimental frequencies for LIM-co-MPAEMA

shown in Fig. 5. Correlation graphic between the observed and calculated ^{1}H chemical shift is drawn in Fig. 6. The squared root correlation factor (R^2) for ^{1}H was calculated to be 0.9713. Experimental shifts of the prepared in chloroform solvent are observed as follows: ^{1}H-NMR spectrum, NH structure at 7.3 ppm, ring protons at 6.9–7.5 ppm, O-CH_3 protons at 3.9 ppm, endocyclic–exocyclic –CH cyclohexene protons 4.9–4.6 ppm, CH cyclohexene 1.3 ppm, CH_2 cyclohexene 2.2–1.8 ppm and polymer chain –CH_2 1.5 ppm. Theoretical chemical shifts are calculated in the ranges 0.9–7.5 ppm. Except for 8H, 12H, 7H, 28H, 24H and 31H atoms, it seems that there is a general conformity between experimental and theoretical results. These atoms were affected by electronegative atoms such as oxygen and nitrogen in their surroundings and showed a higher shift in ppm. The formation of the copolymer can be identified by comparing the ^{1}H-NMR spectrum of the monomer MPAEMA and its D-limonene copolymer. ^{1}H-NMR spectrum of the monomer MPAEMA revealed two multiples in the range of the 5.7–5.6 and 4.5–4.6 ppm olefinic protons (1H, CH and 2H, CH_2). As seen in the ^{1}H-NMR spectrum of LIM-co-MPAEMA (Fig. 5), olefinic protons in the range of 5.7–4.6 ppm are not observed. Also, ^{13}C and ^{1}H chemical shifts are nearly the same for all solvent. So the molecule may not be affected by the solvents.

GPC and thermal characterization of LIM-co-MPAEMA

Molecular weight and molecular weight distribution of copolymer were detected by GPC. The highest molecular weight of the LIM-co-MPAEMA [weight-average molecular weight (M_w) = 44,789, number-average molecular weight (M_n) = 23,687]

Table 2 Comparison of the selected experimental and theoretical vibrational frequencies of LIM-co-MPAEMA

Frequencies (cm^{-1})	B3LYP/6-311++G(d,p)	Experimental
Γ_{tors} COCC(61), Γ_{tors} CCCO(17)	9	
Γ_{tors} CNCC(11), Γ_{tors} CCCC(14)	14	
Γ_{tors} CCCC(17), Γ_{tors} CNCC(37)	23	
Γ_{tors} CNCC(17), Γ_{tors} CCCO(14)	28	
δ_{bend}COC(12), δ_{bend}CCN(12), Γ_{tors} CCCO(17)	34	
Γ_{tors} OCCN(17)	42	
Γ_{tors} CCCC(17), Γ_{tors} CNCC(17), Γ_{tors} COCC(17)	48	
Γ_{tors} CCCC(38), Γ_{tors} CCCO(17)	53	
Γ_{tors} CCCC(17), Γ_{tors} CCCO(12)	59	
Γ_{tors} COCC(10)	74	
Γ_{tors} COCC(29)	85	
Γ_{tors} CCCC(39)	107	
Γ_{tors} COCC(69)	124	
δ_{bend}CNC(12), δ_{bend}NCC(15)	151	
δ_{bend}CCC(14)	159	
δ_{bend}CCC(10)	164	
δ_{bend}CCC(15)	169	
Γ_{tors} CCCC(39), Γ_{tors} CCNC(23)	170	
Γ_{tors} HCCC(67)	193	
Γ_{tors} HCCC(23)	203	
Γ_{tors} HCCC(39)	206	
δ_{bend}CCC(10)	216	
δ_{bend}CCC(10), Γ_{tors} CCCC(39)	221	
Γ_{tors} HCCC(39)	224	
δ_{bend}OCC(10)	230	
Γ_{tors} HCCC(39)	242	
δ_{bend}OCC(11), δ_{bend}COC(12)	259	
Γ_{tors} HCOC(68)	263	
δ_{bend}CCC(30)	278	
Γ_{tors} HCCC(18), Γ_{tors} CCCC(18)	299	
Γ_{tors} HCCC(58)	319	
δ_{bend}COC(14), δ_{bend}CCO(12)	333	
δ_{bend}CCC(12), υCCCC(12)	347	
δ_{bend}CCC(33)	356	
δ_{bend}CCC(46)	364	
δ_{bend}OCN(16), δ_{bend}NCC(24), δ_{bend}COC(12)	386	
δ_{bend}CCC(31)	398	
Γ_{tors} CCCC(31), υOCCC(21), υNCCC(20)	410	
δ_{bend}CCC(13), υCCCC(23)	418	
δ_{bend}CCC(12)	425	
Γ_{tors} CCCC(75), Γ_{tors} HCCC(22)	444	

Table 2 (continued)

Frequencies (cm^{-1})	B3LYP/6-311++G(d,p)	Experimental
ϒCCCC(32)	480	
δ_{bend}CCC(11)	483	
δ_{bend}CCC(13)	493	
δ_{bend}CCC(23)	525	
δ_{bend}CCC(10), δ_{bend}OCC(15), δ_{bend}COC(24)	536	
δ_{bend}CCC(24)	544	
Γ_{tors} CCCC(10), ϒOCNC(31)	565	
δ_{bend}CCN(14), δ_{bend}CCO(21)	340	
Γ_{tors} HNCC(18), Γ_{tors} HCOC(38), ϒOCNC(45)	603	
γ_{str}CC(11), δ_{bend}OCO(14)	617	
δ_{bend}CCC(10)	631	
Γ_{tors} HNCC(71), ϒOCNC(17)	677	
δ_{bend}CCC(16), δ_{bend}OCC(12)	713	
γ_{str}CC(13), δ_{bend}CCC(12)	721	
Γ_{tors} HCCC(38), ϒOCCC(49), ϒNCCC(49)	732	
γ_{str}CC(34)	750	
γ_{str}CC(12), ϒOCOC(49)	751	
γ_{str}OC(19), δ_{bend}CCC(18)	762	
Γ_{tors} HCCC(13)	773	776
Γ_{tors} HCCC(81)	800	
Γ_{tors} HCCC(45), Γ_{tors} HCCC(11)	808	
γ_{str}CC(31)	818	
Γ_{tors} HCCC(46), Γ_{tors} HCCN(29), ϒOCCC(12)	828	829
γ_{str}CC(11), δ_{bend}CCC(18)	854	
γ_{str}CC(32)	859	
Γ_{tors} HCCC(18)	863	
γ_{str}OC(11), γ_{str}CC(25)	868	
Γ_{tors} HCCC(73), Γ_{tors} CCCC(22)	890	
δ_{bend}CCC(16), Γ_{tors} HCCC(14)	894	
Γ_{tors} HCCC(15)	914	
γ_{str}CC(24), Γ_{tors} HCCC(22)	917	
γ_{str}NC(12)	921	
γ_{str}CC(15)	922	
Γ_{tors} HCCC(23), Γ_{tors} HCCN(57)	945	
δ_{bend}HCO(15), Γ_{tors} HCOC(45), ϒOCNC(24)	951	
δ_{bend}CCC(12)	953	
γ_{str}OC(29)	958	960
δ_{bend}HCH(76)	963	
γ_{str}CC(19), γ_{str}OC(18)	969	
Γ_{tors} HCCC(26)	977	
γ_{str}CC(19)	991	
Γ_{tors} HCCC(32)	993	

Table 2 (continued)

Frequencies (cm^{-1})	B3LYP/6-311++G(d,p)	Experimental
γ_{str}CC(10),γ_{str}OC(73)	1024	
γ_{str}CC(10)	1034	1030
γ_{str}CC(10)	1054	
γ_{str}CC(13)	1055	
γ_{str}CC(27), δ_{bend}HCC(37)	1066	
γ_{str}OC(28)	1079	
δ_{bend}HCH(27), Γ_{tors} HCOC(73)	1091	
γ_{str}CC(28), δ_{bend}CCC(10)	1095	
δ_{bend}HCC(33)	1099	
γ_{str}CC(14), Γ_{tors} HCCC(16)	1110	
δ_{bend}HCC(72)	1120	
δ_{bend}HCH(16),Γ_{tors} HCOC(61)	1123	1134
δ_{bend}HCC(21), Γ_{tors} HCCC(10)	1149	
γ_{str}CC(11), Γ_{tors} HCCC(20)	1150	
γ_{str}NC(31), γ_{str}CC(15)	1159	
δ_{bend}HCC(23)	1163	
δ_{bend}HCO(79), Γ_{tors} HCOC(11)	1170	1169
γ_{str}CC(11), γ_{str}OC(17)	1174	
δ_{bend}HCC(35), Γ_{tors} HCCC(21)	1192	
γ_{str}OC(24), γ_{str}NC(12), δ_{bend}HNC(16)	1209	
δ_{bend}HCC(14), Γ_{tors} HCCC(10), Γ_{tors} HCCH(26)	1224	
δ_{bend}HCC(32), Γ_{tors} HCCC(10)	1229	
δ_{bend}COC(22)	1240	1236
δ_{bend}HCC(70)	1247	
δ_{bend}HCC(19), Γ_{tors} HCCC(15)	1253	
δ_{bend}HCC(12)	1254	
γ_{str}CC(11), δ_{bend}HCC(12)	1255	
δ_{bend}HCC(20), Γ_{tors} HCCC(15)	1276	
δ_{bend}HCH(15),Γ_{tors} HCOC(10)	1283	
δ_{bend}HCC(12), Γ_{tors} HCCC(11)	1292	
δ_{bend}HCC(10)	1300	1300
δ_{bend}HCC(15), Γ_{tors} HCCH(15)	1306	
δ_{bend}HCH(59)	1313	
Γ_{tors} HCCC(16)	1315	
δ_{bend}HCH(79)	1321	
δ_{bend}HCH(33), Γ_{tors} HCCC(16)	1324	
δ_{bend}HCH(87)	1334	
γ_{str}CC(40)	1353	
δ_{bend}HCH(83)	1379	
δ_{bend}HCH(67)	1381	
δ_{bend}HCH(35)	1384	
δ_{bend}HCH(37)	1384	

Table 2 (continued)

Frequencies (cm^{-1})	B3LYP/6-311++G(d,p)	Experimental
δ_{bend}HCH(79)	1385	
δ_{bend}HCH(70), Γ_{tors} HCOC(10)	1388	
δ_{bend}HCH(59)	1393	
δ_{bend}HCH(76), Γ_{tors} HCOC(16)	1395	
δ_{bend}HCH(35)	1395	
δ_{bend}HCH(33)	1395	
δ_{bend}HCH(58)	1400	
δ_{bend}HCH(56)	1403	
δ_{bend}HCH(46)	1406	
δ_{bend}HCH(45)	1406	
δ_{bend}HCH(68)	1410	
δ_{bend}HCH(42)	1418	1415
δ_{bend}HCC(59), δ_{bend}CCC(12)	1441	1442
γ_{str}NC(13), δ_{bend}HNC(39)	1467	1464
γ_{str}CC(42), δ_{bend}HNC(15), δ_{bend}CCC(10)	1523	1512
γ_{str}CC(64)	1550	1538
γ_{str}CC(72)	1614	1603
γ_{str}OC(82)	1633	1678
γ_{str}OC(90)	1673	1736
γ_{str}CH(82)	2789	
γ_{str}CH(89)	2790	
γ_{str}CH(97)	2800	
γ_{str}CH(89)	2803	
γ_{str}CH(93)	2805	
γ_{str}CH(96)	2809	
γ_{str}CH(91)	2816	
γ_{str}CH(86)	2825	
γ_{str}CH(89)	2826	
γ_{str}CH(77)	2828	
γ_{str}CH(89)	2832	
γ_{str}CH(81)	2836	2836
γ_{str}CH(87)	2843	
γ_{str}CH(100)	2847	
γ_{str}CH(90)	2855	
γ_{str}CH(99)	2859	
γ_{str}CH(95)	2866	
γ_{str}CH(99)	2872	
γ_{str}CH(88)	2890	
γ_{str}CH(92)	2891	
γ_{str}CH(85)	2894	
γ_{str}CH(95)	2897	
γ_{str}CH(90)	2904	

Table 2 (continued)

Frequencies (cm^{-1})	B3LYP/6-311++G(d,p)	Experimental
γ_{str}CH(90)	2906	
γ_{str}CH(99)	2915	
γ_{str}CH(94)	2916	
γ_{str}CH(98)	2922	
γ_{str}CH(92)	2929	2938
γ_{str}CH(97)	2949	
γ_{str}CH(98)	2983	
γ_{str}CH(97)	2997	
γ_{str}CH(98)	3028	
γ_{str}NH(100)	3368	3317

υ stretching δ: in-plane bending γ: out-of-plane bending Γ: torsion

was determined, and polydispersity index (PDI) of LIM-co-MPAEMA (Mw/Mn) = 1.890 was detected by GPC based on polystyrene standards. All the values shown that limonene can be successfully copolymerized with MPAEMA via free radical route. GPC plots of LIM-co-MPAEMA are shown in Fig. 7.

The thermal properties of LIM-co-MPAEMA were determined by thermal gravimetric analysis (TGA). The initial decomposition temperature (IDT) and the temperature at 50% weight loss are taken as a measure of thermal stability. It has been observed that degradation from the thermogram occurs at two levels. Important values for copolymer of limonene with MPAEMA are: Initial decomposition temperature is 258 °C, decomposition temperature at 30% is 346 °C, decomposition temperature at 50% is 363 °C, weight loss at 300 °C is 17%, weight loss at 450 °C is 65%, and residue at 450 °C and 500 °C is 10% and 0%, respectively. Also, the first maximum decomposition temperature is 357 °C and the second maximum decomposition temperature is 437 °C. The TGA curve of the copolymer is given in Fig. 8.

Frontier molecular orbitals analysis

The frontier molecular orbitals (FMOs) were calculated by B3LYP/6-311++G(d,p) method in DMF, acetonitrile and chloroform solutions. HOMO–LUMO shapes of the studied polymer are given in Fig. 9. The energy gap which is the energy difference between HOMO and LUMO orbital is a critical parameter in measuring the electron conductivity and molecular reactivity. This value is the same for the three solvents and is 5.2 eV as shown in Table 4. 5.2 eV gap (238.6 nm) is in the UV-C region when considering light absorption and is suitable for stable and organic

Table 3 Experimental and calculated chemical shifts (ppm) for LIM-co-MPAEMA

Atom	B3LYP/6-311G++(d,p)			Experimental
	DMF	Acetonitrile	Chloroform	Chloroform
20-C	185	185	184	
13-C	169	169	168	
1-C	163	163	163	
48-C	144	144	144	
4-C	137	137	137	
45-C	127	127	127	
2-C	123	123	124	
3-C	123	123	123	
5-C	123	123	122	
6-C	113	113	112	
15-C	67	67	67	
25-C	55	55	54	
22-C	51	51	51	
21-C	50	50	50	
38-C	45	45	45	
60-C	38	38	38	
40-C	35	35	35	
42-C	35	35	35	
34-C	30	30	30	
39-C	25	25	25	
51-C	24	24	24	
30-C	23	23	23	
56-C	16	16	16	
8-H	8.9	8.9	9.0	7.5
12-H	8.3	8.3	8.1	7.4
7-H	7.2	7.2	7.2	6.9
9-H	7.2	7.2	7.0	7.3
10-H	6.9	6.9	6.8	6.9
50-H	5.7	5.7	5.6	4.9
16-H	4.4	4.4	4.4	4.9
17-H	4.4	4.4	4.4	4.9
28-H	4.1	4.1	4.1	3.9
27-H	3.7	3.7	3.7	3.9
26-H	3.7	3.7	3.7	3.9
46-H	2.2	2.2	2.2	1.8
24-H	2.2	2.2	2.1	1.5
49-H	1.8	1.8	1.8	1.8
47-H	1.8	1.8	1.8	1.8
55-H	1.8	1.8	1.8	1.8
54-H	1.6	1.6	1.6	1.8
44-H	1.6	1.6	1.5	1.8
37-H	1.6	1.6	1.5	1.5

Table 3 (continued)

Atom	B3LYP/6-311G++(d,p)			Experimental
	DMF	Acetonitrile	Chloroform	Chloroform
52-H	1.5	1.5	1.5	1.8
33-H	1.4	1.4	1.5	1.4
53-H	1.4	1.4	1.4	1.8
41-H	1.3	1.3	1.3	1.3
23-H	1.3	1.3	1.3	1.5
32-H	1.2	1.2	1.2	1.4
36-H	1.2	1.2	1.2	1.5
35-H	1.2	1.2	1.2	1.5
43-H	1.2	1.2	1.2	1.8
61-H	1.1	1.1	1.2	1.1
57-H	0.9	0.9	0.9	0.9
58-H	0.9	0.9	0.9	0.9
31-H	0.6	0.6	0.6	1.4
59-H	0.6	0.6	0.6	0.9

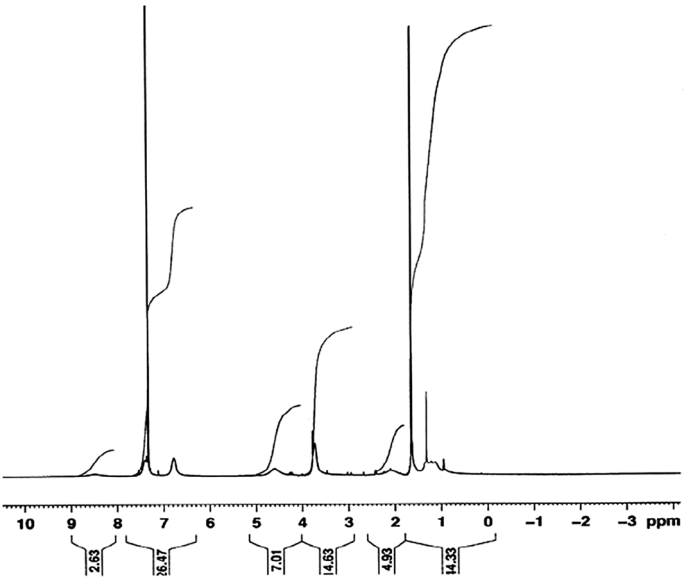

Fig. 5 [1]H-NMR spectrum of LIM-co-MPAEMA

molecules. In addition, energy values of other important HOMO-1 and LUMO + 1 orbitals, which determine parameters such as molecular reactivity and electron

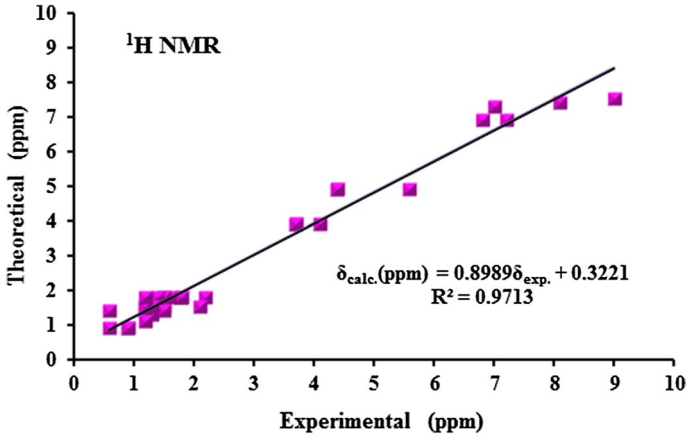

Fig. 6 Correlation graphic between the observed and calculated ^{1}H chemical shift

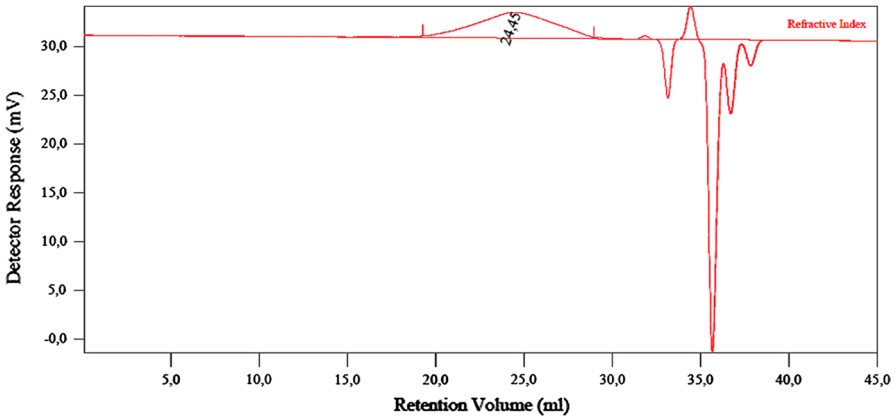

Fig. 7 GPC curve of the LIM-co-MPAEMA

conductivity, are presented in Fig. 9. The value of chemical hardness (h) is 2.6 eV in all solvents. Electronegativity, chemical potential and electrophilicity index are the same for DMF and acetonitrile solvents, but they are different in chloroform solvent.

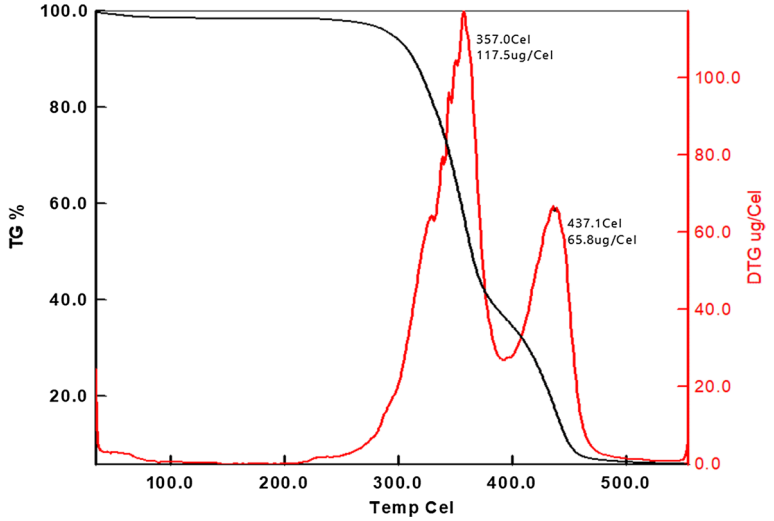

Fig. 8 TGA curves of LIM-co-MPAEMA

Table 5 reports the total electronic energy (E) and global reactivity descriptors (χ, η and μ) for nucleic acid bases, viz. adenine, guanine, cytosine, thymine and uracil. There are always electron flows from less electronegative system to more electronegative system [54]. To quantitatively estimate the electron transfer in the interaction of nucleic acid bases with LIM-co-MPAEMA, we have calculated the amount of charge transfer between LIM-co-MPAEMA and model biomolecules by applying Eq. 1. It is seen that all ΔN values are negative, and thus, LIM-co-MPAEMA acts as an electron donor in its reactions with its receptors. This causes the electron density to drop, and thus, the ability to form a reaction causes the reactivity to decrease.

Total, partial and population density of states (DOS, PDOS and OPDOS)

Molecular orbitals close to each other in a boundary region of a molecule may have semi-degenerate energy levels [55]. Therefore, defining the HOMO–LUMO orbitals is not the true definition of the molecular boundary orbitals. In this context, TDOS, PDOS and OPDOS (or COOP) density of states [56–58] were calculated and formed via GaussSum2.2 program [51/50] by convoluting the molecular orbital information with Gaussian curves of unit height with full width at half maximum (FWHM) of 0.3 eV. TDOS, PDOS and OPDOS graphs are presented in Figs. 10, 11 and 12. Positive, negative and zero values in the OPDOS diagram indicate interactions with

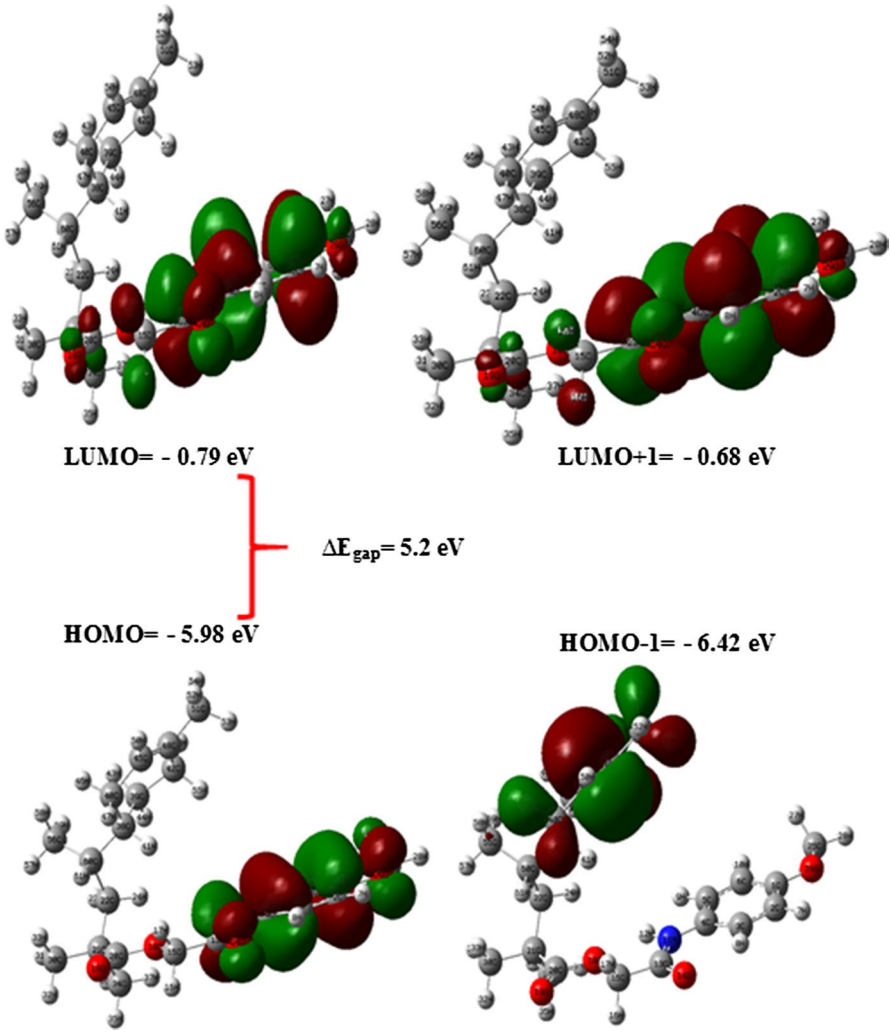

Fig. 9 Frontier molecular orbitals of LIM-co-MPAEMA

bonding, antibonding and non-bonding, respectively [58]. In addition, with the OPDOS diagram, it helps to identify orbitals that do binding and non-binding and at the same time to determine the donor–acceptor properties of the ligand. Figure 12 denotes some

Table 4 Calculated energies values for LIM-co-MPAEMA

	Dmf	Acetonitrile	Chloroform
E_{total} (Hartree)			
E_{HOMO} (eV)	−6.01	−6.01	−5.98
E_{LUMO} (eV)	−0.81	−0.81	−0.79
E_{HOMO-1} (eV)	−6.43	−6.43	−6.42
E_{LUMO+1} (eV)	−0.71	−0.71	−0.68
$E_{HOMO-1–LUMO+1\ gap}$ (eV)	−5.72	−5.72	−5.74
$E_{HOMO–LUMO\ gap}$ (eV)	−5.2	−5.2	−5.2
Chemical hardness (h)	2.6	2.6	2.6
Electronegativity (χ)	−3.41	−3.41	−3.38
Chemical potential (μ)	3.41	3.41	3.38
Electrophilicity index (ω)	2.24	2.24	2.20

Table 5 Calculated electronic energy, chemical hardness, chemical potential of LIM-co-MPAEMA molecule and calculated charge transfer between LIM-co-MPAEMA molecule and NA bases

Bases	Electronic energy (eV)	Chemical Hardness (eV)	Chemical Potential (eV)	ΔN
Adenine	−12,720.504	2.68	−3.79	−1.004
Thymine	−12,362.028	2.70	−4.17	−2.004
Guanine	−14,768.821	2.67	−3.51	−0.258
Cytosine	−10,750.465	2.52	−3.92	−1.296
Uracil	−11,291.830	2.80	−4.37	−2.601

of orbitals energy values of the interactions among the selected groups. The interaction between methacrylate and phenylamino is positive and demonstrates bond interaction. The interaction between oxoethyl and methacrylate, oxoethyl and phenylamino and limonene and methacrylate is negative and has antibond interaction. Interactions among the remaining groups are zero, indicating non-binding orbitals.

Conclusion

In this study, a copolymer of limonene with MPAEMA (LIM-co-MPAEMA) was synthesized, characterized by FTIR and ^{1}H NMR spectroscopy techniques. The molecular weight of the copolymer is determined by using GPC and thermal properties of copolymer detected by the TGA. Both experimental and theoretical methods showed that the compound was successfully synthesized. The results showed that the calculated frequencies and chemical shifts correspond to the experimental values. Considering the total thermal characterization and decomposition temperature (258 °C), it can be said that LIM-co-MPAEMA copolymer has thermal stability. Similarly, it appears to be energetically stable with an energy interval of 5.2 eV

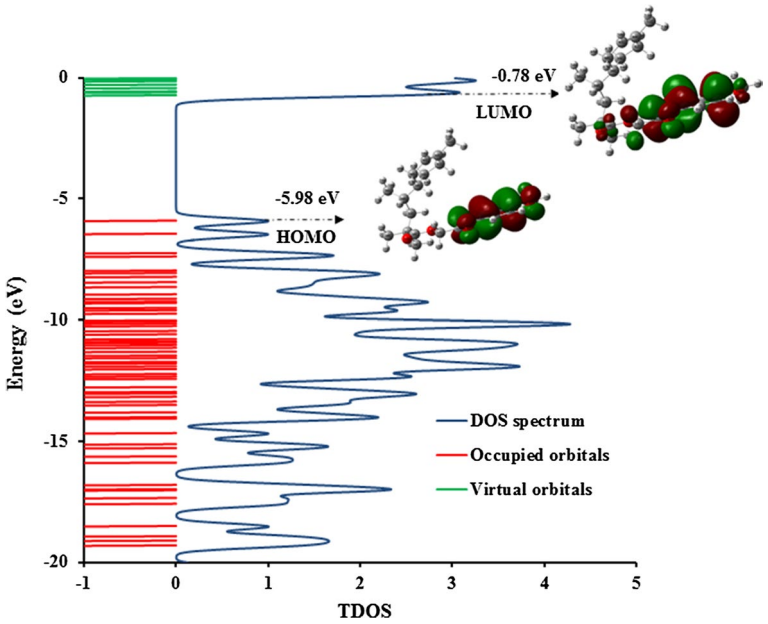

Fig. 10 Total electronic density of states diagram of LIM-co-MPAEMA

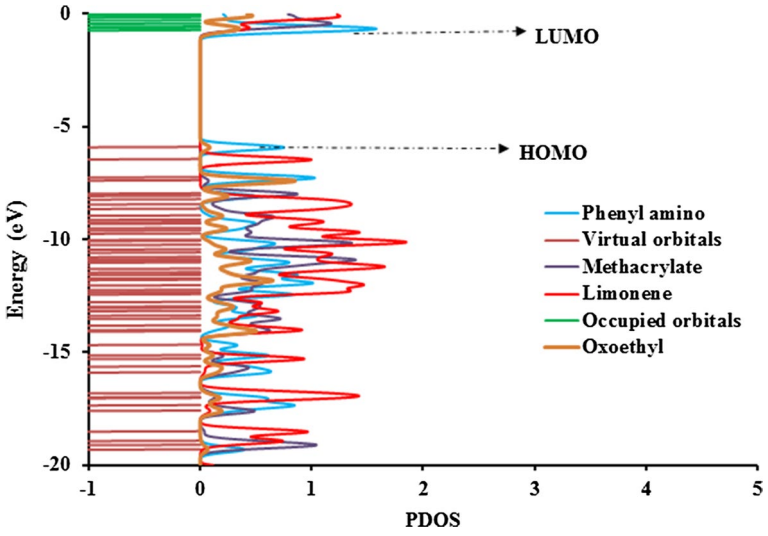

Fig. 11 Partial electronic density of states diagram of LIM-co-MPAEMA

determined by HOMO–LUMO analysis. In addition, this polymer can be used as a biomaterial since it behaves as an electron donor when compared with a biosystem.

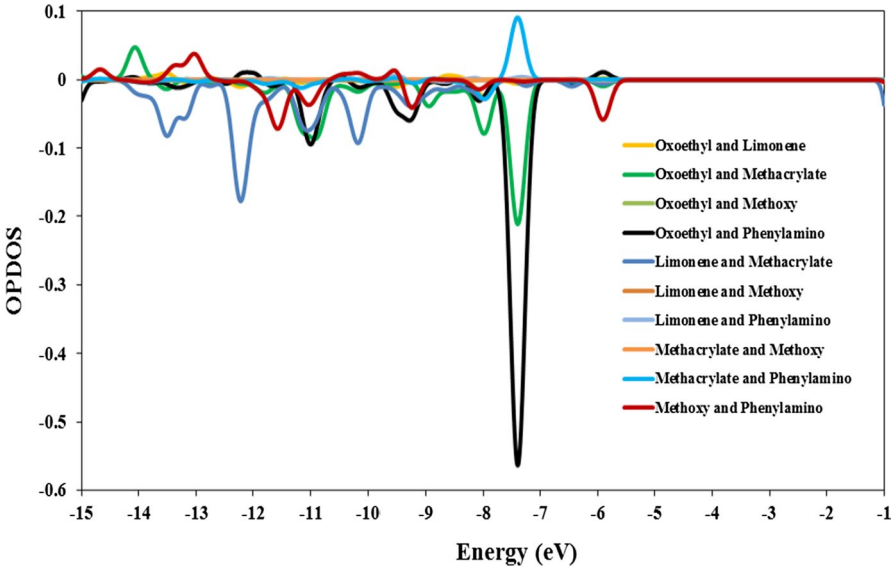

Fig. 12 Overlap population electronic density of states diagram of LIM-co-MPAEMA

References

1. Odian G (2004) Principles of polymerization. Wiley, Hoboken
2. Kerton FM, Marriott R (2013) Alternative solvents for green chemistry. In: Clark JH, Kraus G, Stankiewicz A (eds) Renewable solvents, vol 20. Royal Society of Chemistry, Cambridge, p 97
3. Kim YW, Kim MJ, Chung BY, Bang DY, Lim SK, Choi SM, Lim DS, Cho MC, Yoon K, Kim HS, Kim KB, Kim YS, Kwack SJ, Lee B (2013) Safety evaluation and risk assessment of D-limonene. J Toxicol Environ Health B 16:17
4. Filipsson AF, Bard J, Karlsson S (1998) Concise international chemical assessment document 5: limonene. World Health Organization, Geneva, p 1
5. Bauer K, Garbe D (2006) Surburg H. In: Bauer K (ed) Common fragrance and flavor materials: preparation, properties and uses. Wiley, Weinheim, p 330
6. Breitmaier E (2006) Terpenes: importance, general structure, and biosynthesis. Wiley, Weinheim, p 1
7. Gu Y, Jerome F (2013) Bio-based solvents: an emerging generation of fluids for the design of eco-efficient processes in catalysis and organic chemistry. Chem Soc Rev 42:9550
8. Mohammad A (ed) (2012) Green solvents. I, properties and application in chemistry. Springer, New York **(eds: Inamuddin)**
9. Modena M, Bates RB, Marvel CS (1965) Some low molecular weight polymers of D-limonene and related terpenes obtained by Ziegler-type catalyst. J Polym Sci A 3:949–960
10. Roberts WJ, Day AR (1950) Study of the polymerization of a-pinene and b-pinene with Friedal–Craft catalyst. J Am Chem Soc 72:1226–1230
11. Doiuchi T, Yamaguchi H, Minoura Y (1981) Cyclocopolymerization of d-limonene with maleic anhydride. Eur Polym J 17(9):961
12. Sharma S, Srivastava A (2004) Synthesis and characterization of copolymers of limonene with styrene initiated by azobisisobutyronitrile. Eur Polym J 9:2235–2240
13. Sharma S, Srivastava A (2003) Radical copolymerization of limonene with acrylonitrile: kinetics and mechanism. Polym Plast Technol Eng 3:485–502
14. Sharma S, Srivastava A (2003) Alternating copolymers of limonene with methyl methacrylate: kinetics and mechanism. J Appl Polym Sci 6:593–603

15. Zhang Y, Dube AM (2015) Copolymerization of 2-ethylhexyl acrylate and dlimonene, copolymerization of 2-ethylhexyl acrylate and D-limonene. Polym Plast Technol Eng 54(5):499–505
16. Kindermann N, Cristofol A, Kleij AW (2017) Access to biorenewable polycarbonates with unusual glass-transition temperature (T_g) modulation. ACS Catal 7(6):3860–3863
17. Nendza M, Volmer J, Klein W, Kalcher N, Devillers J (eds) (1990) Risk assessment based on QSAR estimates. Kluwer Academic Publishers, Dordrecht, pp 213–240
18. Schultz TW (1997) Tetrahymena pyriformis population growth impairment endpointa surrogate for fish lethality. Toxicol Methods 7:289–309
19. Dimitrov SD, Mekenyan OG, Schultz TW (2000) Interspecies modeling of narcotics toxicity to aquatic animals. Bull Environ Contam Toxicol 65:399–406
20. Chattaraj PK, Nath S, Maiti B (2003) Reactivity descriptors. In: Tollenaere J, Bultinck P, Winter HD, Langenaeker W (eds) Computational medicinal chemistry for drug discovery, chap 11. Marcel Dekker, New York, pp 295–322
21. Parthasarathi R, Padmanabhan J, Subramanian V, Maiti B, Chattaraj PK (2003) Molecular structure, reactivity, and toxicity of the complete series of chlorinated benzenes. J Phys Chem A 107:13046
22. Parthasarathi R, Padmanabhan J, Subramanian V, Maiti B, Chattaraj PK (2004) Toxicity analysis of 33′44′5-pentachloro biphenyl through chemical reactivity and selectivity profiles. Curr Sci 86:535–542
23. Padmanabhan J, Parthasarathi R, Sarkar U, Subramanian V, Chattaraj PK (2004) Effect of solvation on the condensed Fukui function and the generalized philicity index. Chem Phys Lett 383(1–2):122–128
24. Roy RK, De Proft F, Geerlings P (1998) Site of protonation in aniline and substituted anilines in the gas phase: a study via the local hard and soft acids and bases concept. J Phys Chem A 102:7035
25. Mendez F, Tamariz J, Geerlings P (1998) 1, 3-dipolar cycloaddition reactions: a DFT and HSAB principle theoretical model. J Phys Chem A 102:6292
26. Langenaeker W, De Proft F, Geerlings P (1998) Ab initio and density functional theory study of the geometry and reactivity of benzyne, 3-fluorobenzyne, 4-fluorobenzyne, and 4, 5-didehydropyrimidine. J Phys Chem A 102:5944
27. Roy RK, Krishnamurthy S, Geerlings P, Pal S (1998) Local softness and hardness based reactivity descriptors for predicting intra-and intermolecular reactivity sequences: carbonyl compounds. J Phys Chem A 102:3746
28. Chatterjee A, Iwasakı T, Ebina T (1999) Reactivity index scale for interaction of heteroatomic molecules with zeolite framework. J Phys Chem A 103:2489
29. Perez P, Toro-Labbe A, Contreras R (1999) HSAB analysis of charge transfer in the gas-phase acid–base equilibria of alkyl-substituted alcohols. J Phys Chem A 103:11246
30. Jaque P, Toro-Labbe A (2000) Theoretical study of the double proton transfer in the CHX–XH⊙⊙⊙ CHX–XH (X = O, S) complexes. J Phys Chem A 104:995
31. Perez P, Toro-Labbe A, Contreras R (2000) Global and local analysis of the gas-phase acidity of haloacetic acids. J Phys Chem A 104:5882
32. Gutıerrez-Oliva S, Jaque P, Toro-Labbe A (2000) Using Sanderson's principle to estimate global electronic properties and bond energies of hydrogen-bonded complexes. J Phys Chem A 104:8955
33. Parthasarathi R, Padmanabhan J, Sarkar U, Maiti B, Subramanian V, Chattaraj PK (2003) Toxicity analysis of benzidine through chemical reactivity and selectivity profiles: a DFT approach. Internet Electron J Mol Des 2:798–813
34. Roy DR, Parthasarathi R, Maiti B, Subramanian V, Chattaraj PK (2005) Electrophilicity as a possible descriptor for toxicity prediction. Bioorg Med Chem 13:3405–3412
35. Kloosterboer JG (1988) Network formation by chain crosslinking photopolymerization and its applications in electronics. Adv Polym Sci 84:1
36. Matyjaszewski K, Gnanou Y, Leibler L (2007) Macromolecular engineering: precise synthesis, materials properties, applications. Wiley, Weinheim
37. Ljubic TS, Pahovnik D, Žigon M, Žagar E (2012) Photochemically active systems and probes for polymer research. Sci World J 2012:1
38. Acikbas Y, Cankaya N, Capan R, Erdogan M, Soykan C (2016) Swelling behaviour of the 2-(4-methoxyphenylamino)-2-oxoethyl methacrylate monomer LB thin film exposed to various organic vapours by quartz crystal microbalance technique. J Macromol Sci A Pure Appl Chem 53(1):18–25

39. Gülbaş HE, Çankaya N (2017) D-Limonen İle 2-(4-Metoksifenilamino)-2-Oksoetil Metakrilat (MPAEMA) Kopolimerinin (Limonen-co-MPAEMA) Sentezi ve Karakterizasyonu. In: 2nd international congress on engineering architecture and design, oral presentation, Kocaeli-Turkey, pp 749–750
40. Kohn W, Sham LJ (1965) Self-consistent equations including exchange and correlation effects. Phys Rev 140:A1133–A1138
41. Becke AD (1988) Density-functional exchange-energy approximation with correct asymptotic behavior. Phys Rev A 38:3098–3100
42. Vosko SH, Vilk L, Nusair M (1980) Accurate spin-dependent electron liquid correlation energies for local spin density calculations: a critical analysis. Can J Phys 58:1200–1211
43. Lee C, Yang W, Parr RG (1988) Development of the Colle–Salvetti correlation-energy formula into a functional of the electron density. Phys Rev B 37:785–789
44. Frisch MJ et al (2009) Gaussian 09, revision A.1. Gaussian, Inc., Wallingford
45. http://cccbdb.nist.gov/vsfx.asp
46. Jamroz MH (2013) Vibrational energy distribution analysis (VEDA): scopes and limitations. Spectrochim Acta A Mol Biomol Spectrosc 114:220–230
47. Parr RG, Pearson RG (1983) Absolute hardness: companion parameter to absolute electronegativity. J Am Chem Soc 105:7512–7516
48. Ditchfield R (1972) Molecular orbital theory of magnetic shielding and magnetic susceptibility. J Chem Phys 56:5688–5691
49. Wolinski K, Hinton JF, Pulay P (1990) Efficient implementation of the gauge-independent atomic orbital method for NMR chemical shift calculations. J Am Chem Soc 112:8251–8260
50. O'Boyle NM, Tenderholt AL, Langner KM (2008) Cclib: a library for package-independent computational chemistry algorithms. J Comput Chem 29:839–845
51. Abraham CS, Prasana JC, Muthu S (2017) Quantum mechanical, spectroscopic and docking studies of 2-amino-3-bromo-5-nitropyridine by density functional method. Spectrochim Acta A 181:153–163
52. Socrates G (2001) Infrared and Raman characteristics group frequencies, tables and charts, 3rd edn. Wiley, Chichester
53. Sundaraganesan N, Illakiamani S, Meganathan C, Joshua BD (2007) Vibrational spectroscopy investigation using ab initio and density functional theory analysis on the structure of 3-aminobenzotrifluoride. Spectrochim Acta A 67:214–224
54. Fukui K (1982) Role of frontier orbitals in chemical reactions. Science 218:747–754
55. Tanış E, Babur Şaş E, Kurban M, Kurt M (2017) The structural, electronic and spectroscopic properties of 4FPBAPE molecule: experimental and theoretical study. J Mol Struct 1154:301–318
56. Hughbanks T, Hoffmann R (1983) Chains of trans-edge-sharing molybdenum octahedra: metal–metal bonding in extended systems. J Am Chem Soc 105:3528–3537
57. Małecki JG (2010) Synthesis, crystal, molecular and electronic structures of thiocyanate ruthenium complexes with pyridine and its derivatives as ligands. Polyhedron 29:1973–1979
58. Chen M, Waghmare UV, Friend CM, Kaxiras E (1998) A density functional study of clean and hydrogen-covered α-MoO3(010):α-MoO3(010): electronic structure and surface relaxation. J Chem Phys 109:6854–6860